NMR Stratagems for the Study of Multiple Kinetic Hydrogen/Deuterium Isotope Effects of Proton Exchange. Example: Di-p-fluorophenylformamidine/THF

Hans-Heinrich Limbach, Ludger Meschede, and Gerd Scherer

Institut für Physikalische Chemie der Universität Freiburg i. Br., West Germany

Z. Naturforsch. **44a**, 459–472 (1989); received January 25, 1989

Dedicated to Professor Jacob Bigeleisen on the occasion of his 70th birthday

Stratagems are presented for the determination of kinetic isotope effects of proton exchange reactions by dynamic NMR spectroscopy. In such experiments, lineshape analyses and/or polarization transfer experiments are performed on the exchanging protons or deuterons as well as on remote spins, as a function of the deuterium fraction in the mobile proton sites. These methods are NMR analogs of previous proton inventory techniques involving classical kinetic methods. A theory is developed in order to derive the kinetic isotope effects as well as the number of transferred protons from the experimental NMR spectra. The technique is then applied to the problem of proton exchange in the system $^{15}N,^{15}N'$-di-p-fluorophenylformamidine, a nitrogen analog of formic acid, dissolved in tetrahydrofuran-d_8 (THF). DFFA forms two conformers in THF to which s-trans and s-cis structures have been assigned. Only the s-trans conformer is able to dimerize and exchange protons. Lineshape simulations and magnetization transfer experiments were carried out at 189,2 K, at a concentration of 0.02 mol l^{-1}, as a function of the deuterium fraction D in the ^1H-^{15}N sites. Using ^1H NMR spectroscopy, a linear dependence of the inverse proton lifetimes on D was observed. From this it was concluded that two protons are transported in the rate limiting step of the proton exchange. This result is expected for a double proton transfer in an s-trans dimer with a cyclic structure. The full kinetic HH/HD/DD isotope effects of 233:11:1 at 189 K were determined through ^{19}F NMR experiments on the same samples. The deviation from the rule of geometric mean, although substantial, is much smaller than found in previous studies of intramolecular HH transfer reactions. Possible causes of this effect are discussed.

Key words: NMR spectroscopy (dynamic), Proton exchange, Isotope effects (kinetic HH/HD/DD), Formamidine, Hydrogen bonding.

1. Introduction

A number of chemical reactions involve the transfer of $m=1$ or more protons, hydrogen atoms or hydride ions in the rate limiting step [1–3], which leads to kinetic hydrogen/deuterium isotope effects on the reaction rates. It is obvious that the knowledge of both m and the kinetic isotope effects is important for an understanding of the mechanisms of these reactions. It has long been known that both quantities can be determined by measuring reaction rates as a function of the deuterium fraction D in the mobile proton sites [1, 6–8]. This method, called "proton inventory technique", has been applied to a number of organic and biochemical reactions [1–13] in protic media. Unfortunately, if $m>1$ a proton inventory plot depends on more parameters than can easily be obtained by non-linear regression analysis of the kinetic data, a situation which makes certain assumptions necessary. Thus, the validity of the "rule of the geometric mean" (RGM) has often been assumed. For the isotopic rate constants of a double proton transfer reaction of the type

$$AH + XH^* \rightleftharpoons [AH, XH^*] \rightleftharpoons [AH^*, XH] \rightleftharpoons AH^* + XH. \quad (1)$$

the RGM states that

$$k^{HD} = (k^{HH}\, k^{DD})^{1/2}, \quad \text{i.e.} \quad k^{HH}/k^{HD} = k^{HD}/k^{DD}. \quad (2)$$

This rule has been derived from a combination of transition state theory [14] and equilibrium isotope fractionation theory [7, 15–19]. The latter theory, which has frequently been verified, relates the equilibrium constants of isotopic reactions to the set of vibrational frequencies of the educts and products. By contrast, the problem of calculating kinetic isotope effects

Reprint requests to Prof. Dr. H.-H. Limbach, Institut für Physikalische Chemie der Universität Freiburg i. Br., Albertstr. 21, D-7800 Freiburg i. Br., West Germany.

0932-0784 / 89 / 0500-0459 $ 01.30/0. – Please order a reprint rather than making your own copy.

still remains because the vibrational frequencies of transition states cannot be observed spectroscopically and because of proton tunneling, which also affects kinetic hydrogen/deuterium isotope effects [1].

In order to check the validity of the RGM we have, for a number of years, been studying kinetic isotope effects of well characterized multiple symmetric proton transfer reactions by dynamic NMR spectroscopy in non aqueous liquids [17, 20–34] and, recently, also in the solid state [35–42]. Large deviations from (2) were observed for the intramolecular HH migrations in meso-tetraphenylporphine [17] and azophenine [17, 32, 33] as well as for proton exchange between acetic acid and methanol in tetrahydrofuran (THF) [17, 21], as replacement of the first H atom by D resulted in a larger decrease in the rate constants than replacement of the second H atom by D. These results have been useful in elucidating kinetic results of enzyme reaction mechanisms [10, 11]. Tunnel contributions to the reaction rates as well as stepwise proton transfer mechanisms [17, 32] have been discussed as causes of the deviations from the RGM.

In order to measure the above mentioned multiple kinetic isotope effects, NMR proton inventory techniques [17, 21, 29, 31, 32] had to be designed that involve dynamic NMR measurements as a function of the deuterium fraction D in the mobile proton sites. When the chemical shifts of the jumping protons or deuterons are altered during the exchange, kinetic constants can be derived by a combination of ^1H and ^2H NMR spectroscopy [17, 21]. Unfortunately, intramolecular proton transfers in symmetric molecules and intermolecular proton self exchange (A = X in (1)) are processes during which the chemical shifts of the jumping hydrogen isotopes are not modulated. The use of the modulation of a scalar spin-spin interaction between the mobile hydrogen isotopes L and "remote" spins in the residual group A of a molecule AL is only a partial solution to the problem because of the following circumstance. Although kinetic HH/HD isotope effects can be obtained from the analysis of A–H splitting patterns by ^1H NMR experiments [17, 28, 29, 31, 33, 34], scalar A–D coupling is not strong enough to obtain kinetic HD/DD isotope effects by ^2H NMR spectroscopy because of the smaller gryomagnetic ratio of the ^2H nucleus. Therefore, kinetic HH/DD isotope effects of several intramolecular double proton transfer reactions were obtained by performing NMR experiments on remote spins such as ^{13}C [17, 33]. Remote spins do not directly participate

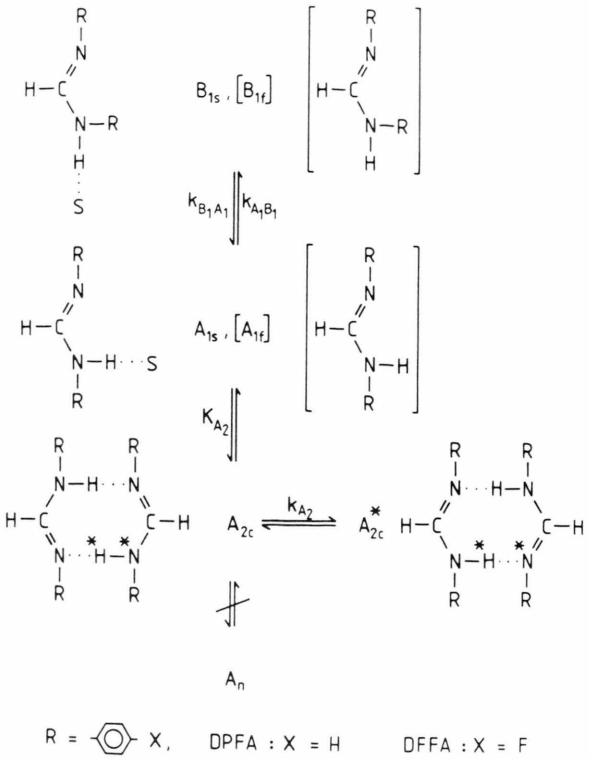

Fig. 1. Exchange processes of N,N′-diarylamidines in THF as identified by NMR spectroscopy [31]. The species in square brackets were identified only indirectly.

in the exchange but their chemical shifts are modulated by the latter.

So far, remote spin NMR proton inventories for the determination of kinetic isotope effects of intermolecular proton self exchange between like molecules AL have not yet been described. The purpose of this paper is to give such a description and to show that such experiments can be very useful. The theoretical section deals with the kinetic quantities of hydrogen exchange obtained from remote spin experiments. These are defined and compared with those obtainable from experiments on exchanging spins. NMR lineshape equations are set up for some simple spin systems.

As an example, we present results of an NMR study of kinetic isotope effects on the proton exchange of an N,N′-diarylamidine (Figs. 1 and 2) dissolved in tetrahydrofuran (THF). Although the amidines – which represent the nitrogen analogs of carboxylic acids – are very old compounds [44], their physical and chemical properties are not very well known. IR studies of amidines [45, 46] have been interpreted in terms of the

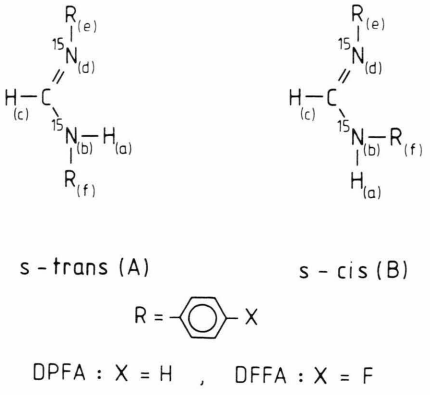

Fig. 2. Atom labeling of $^{15}N,^{15}N'$-di(-fluorophenyl)-formamidine in the s-cis and the s-trans form.

formation of cyclic hydrogen bonded complexes with a structure similar to those of carboxylic acids. The first studies of proton exchange of amidines were performed by Halliday et al. [47] and Borisov et al. [48], but they did neither report rate laws nor kinetic isotope effects. Borisov et al. also reported that N,N'-diarylformamidines exist in tetrahydrofuran (THF) in an s-trans form A and an s-cis form B, which show different exchange characteristics. In a recent dynamic NMR study of $^{15}N,^{15}N'$-dipentadeuterophenylformamidine (DPFA) in THF [31] we have established the complex reaction network shown in Figure 1. The ^{15}N label had to be introduced in order to avoid ^{14}N quadrupole effects on the mobile proton signals, which obscure the kinetic information on proton exchange. The principle results of this study were the following. Only the s-trans isomer A is able to form a cyclic dimer in which a fast double proton transfer takes place. This transfer is characterized by a kinetic HH/HD isotope effect of about 20 at 178 K. Hydrogen bond exchange is extremely fast, the exchange of the two conformers very low on the NMR timescale at this temperature. A non-linear rate law of the proton exchange was found, second order at low and first order at high concentrations, as expected for the reaction network of Figure 1.

In the case of these arylamidines we found it difficult to use ^{13}C or ^{15}N as remote spin labels for the study of the kinetic isotope effects of the proton self exchange because of the bad signal to noise ratio of the NMR spectra of these nuclei. Therefore, we introduced in this study according to Borisov et al. [48] ^{19}F as a more convenient remote spin label for the exchange into the para positions of the phenyl rings of DPFA, which leads to $^{15}N,^{15}N'$-di-p-fluorophenylformamidine (DFFA). Whereas the number $m=2$ of transferred protons in the rate limiting step of the self exchange was obtained by ^1H NMR, the kinetic HH/HD/DD isotope effects could be obtained by ^{19}F NMR spectroscopy.

In the following experimental section we describe the synthesis of DFFA and the experimental conditions. After the theoretical section the results are presented. In the discussion, the kinetic isotope effects of the DFFA proton selfexchange are compared with those obtained previously for other double proton transfer reactions; finally, we propose an explanation for the different behaviour of intramolecular and intermolecular proton transfer systems with respect to the validity of the RGM.

2. Experimental

2.1. Synthesis of $^{15}N,^{15}N'$-di-(4-fluorophenyl)-formamidine (DFFA)

^{15}N labeled DFFA was synthesized in a similar way to that described recently [31] for diphenylformamidine by reaction of 0.095 g (0.892 mmol) triethylorthoformate with 0.2 g (1.784 mmol) p-fluoroaniline-^{15}N. The reaction mixture was kept for 5 h at 40 °C. After recrystallization from n-heptane, a material (0.16 g yield, 76% of the theory) with a melting point of 144.9 °C was obtained (lit. [48]: 141 °C–145 °C).

2.2. Synthesis of p-Fluoroaniline-^{15}N

p-Fluoroaniline-^{15}N was synthesized according to ref. [49] from p-fluorobenzamide-^{15}N and sodium hypobromide via the Hoffmann reaction. First, a solution of sodiumhypobromide was prepared by slowly adding 0.22 ml (4.29 mmol) bromine to an ice-cold stirred solution of 0.766 g (19.16 mmol) sodiumhydroxide in 15 ml water. After 5 minutes, 0.5 g (3.59 mmol) p-fluorobenzamide-^{15}N was added. The reaction mixture was stirred at 0 °C for 20 minutes until a clear yellow solution formed, and then heated slowly in an oil bath to 95 °C, where it was kept for 1.5 hours. After cooling to room temperature, the dark organic phase was extracted three times with 30 ml ether and dried over Na_2SO_4. The ether was then removed and the product purified by evaporation and condensation *in vacuo*. p-Fluoroaniline-^{15}N (0.3 g, 77% of the theoretical yield) was then identified by ^1H- and ^{19}F-NMR-spectroscopy.

2.3. Synthesis of p-Fluorobenzamide-^{15}N

p-Fluorobenzamide-^{15}N was synthesized in a similar way to that described by Axenrod et al. [51] from 2 g (36.7 mmol) $^{15}NH_4Cl$ in 18 ml water and 4.34 ml (36.7 mmol) p-fluorobenzochloride. The melting point of the product (4.37 g, 85% theoretical yield) was 157.3 °C (lit. [50]: 158.0 °C).

2.4. Preparation of Samples

The sealed DFFA NMR samples had to be prepared very carefully on a vacuum line in order to exclude air and moisture and any other impurities that might catalyse the proton exchange. The procedure is similar to that described for DPFA [31]. Since the density of THF is temperature dependent, the concentrations $C(T)$ at temperature T were calculated for each sample using the following equation [52]:

$$C(T)/C(298\text{ K}) = 1 + 9.26 \cdot 10^{-4} \cdot (298 - T). \quad (3)$$

The values of $C(298\text{ K})$ and of the deuterium fraction D in the mobile proton site were checked by ^1H NMR spectroscopy. A 0.25 molar sample was used as a reference.

2.5. NMR Measurements

The 300 MHz ^1H NMR spectra were recorded with a Bruker pulse FT NMR spectrometer MSL 300, the 84.7 MHz ^{19}F NMR spectra with a Bruker CXP 100 pulse FT NMR spectrometer. During the ^{19}F NMR experiments the protons were decoupled using the CW homodecoupling technique, the irradiating frequency being centered on the aromatic protons. For temperature control a Bruker B VT 100 unit was employed. The sample temperatures were checked before and after each experiment with a Pt 100 resistance thermometer (Degussa) embedded in an NMR tube; they are estimated to be accurate to about 0.5 °C. The temperature stability during the measurements was, however, better than 0.2 °C. The spectra were transferred from the Bruker Aspect 2000 minicomputer to a personal computer (Olivetti M 28), and then to the Univac 1108 computer of the Rechenzentrum der Universität Freiburg via a direct data line. Kinetic and thermodynamic parameters were obtained by simulation of the spectra, as described below. Various experimental data were fitted to theoretical curves using a non-linear least squares fit program [53].

3. Theoretical Section

When studying the kinetics of isotopic exchange reactions of molecules AH and AD, one has the option of performing experiments either on the A spins, the H and/or the D spins. The kinetic quantities obtained in the various experiments depend on which nuclear spins are chosen for the experiments. This section is devoted to a description of these quantities. First, we define these quantities as well as their relations to convential kinetics and then derive NMR lineshape equations for some simple spin systems relevant in the context of this study.

3.1. The Relation between Rate Constants of Intermolecular Hydrogen/Deuterium Transfer Reactions and Inverse Lifetimes Measured by NMR Spectroscopy

In order to demonstrate the special features of NMR let us first look at a simple equilibrium

$$i \rightleftharpoons j \quad (4)$$

characterized by the equilibrium constant

$$K_{ij} = k_{ij}/k_{ji} = C_j/C_i\,. \quad (5)$$

C_i and k_{ij} are the usual concentrations and the pseudo first order rate constants. NMR experiments are, generally, performed under equilibrium conditions. The NMR lineshapes depend on the inverse lifetimes

$$\tau_{ij}^{-1} = k_{ij} = -C_i^{-1}\,\mathrm{d}C_{i\to j}/\mathrm{d}t\,. \quad (6)$$

Thus, for the definition of the kinetic quantities one can treat the forward and backward reaction rates separately.

Now, let us consider again a molecule AH and its deuterated analog AD, where H and D are mobile protons and deuterons. Without assuming any reaction mechanism, one can formulate the following group exchange reactions [22] observable by NMR

$$\mathrm{AH} \xrightarrow{\tau_{\mathrm{AHAH^*}}^{-1}} \mathrm{AH^*}, \quad \mathrm{AH} \xrightarrow{\tau_{\mathrm{AHAD}}^{-1}} \mathrm{AD},$$

$$\mathrm{AD} \xrightarrow{\tau_{\mathrm{ADAH}}^{-1}} \mathrm{AH}, \quad \mathrm{AD} \xrightarrow{\tau_{\mathrm{ADAD^*}}^{-1}} \mathrm{AD^*}, \quad (7)$$

$$\mathrm{AH} \xrightarrow{\tau_{\mathrm{AHA^*H}}^{-1}} \mathrm{A^*H}, \quad \mathrm{AD} \xrightarrow{\tau_{\mathrm{ADA^*D}}^{-1}} \mathrm{A^*D}, \quad (8)$$

Here an asterisk is introduced to characterize physically different atomic or molecular species of the same kind. $\tau_{\mathrm{ALAM}}^{-1}$, with LM = HH, HD, DD, represents the pseudo first order exchange rate constant of group A

(marked in boldface) between the environments AL and AM, i.e. the inverse correlation time of group A with spin L before the latter is replaced by spin M. $\tau^{-1}_{\mathbf{ALA^*L}}$ represents the inverse lifetime of the isotope L (marked in boldface) before the transfer from A to the chemically identical, but physically different, environment A* takes place. These lifetimes are defined as follows

$$\begin{aligned}
\tau^{-1}_{\mathbf{AHAH^*}} &= -(1/C_{\mathrm{AH}})\, \mathrm{d}C_{\mathbf{AH\to AH^*}}/\mathrm{d}t,\\
\tau^{-1}_{\mathbf{AHAD}} &= -(1/C_{\mathrm{AH}})\, \mathrm{d}C_{\mathbf{AH\to AD}}/\mathrm{d}t,\\
\tau^{-1}_{\mathbf{ADAH}} &= -(1/C_{\mathrm{AD}})\, \mathrm{d}C_{\mathbf{AD\to AH}}/\mathrm{d}t,\\
\tau^{-1}_{\mathbf{ADAD^*}} &= -(1/C_{\mathrm{AD}})\, \mathrm{d}C_{\mathbf{AD\to AD^*}}/\mathrm{d}t,\\
\tau^{-1}_{\mathbf{AHA^*H}} &\equiv \tau^{-1}_{\mathrm{AH}} = -(1/C_{\mathrm{AH}})\, \mathrm{d}C_{\mathbf{AH\to A^*H}}/\mathrm{d}t,\\
\tau^{-1}_{\mathbf{ADA^*D}} &\equiv \tau^{-1}_{\mathrm{AD}} = -(1/C_{\mathrm{AD}})\, \mathrm{d}C_{\mathbf{AD\to A^*D}}/\mathrm{d}t, \qquad (9)
\end{aligned}$$

It is evident that $\tau^{-1}_{\mathbf{ALAM}}$ can be determined only by lineshape analysis of the remote A-spin spectra. By contrast, the NMR spectra of the mobile L spins depend on the quantity $\tau^{-1}_{\mathbf{ALA^*L}}$. It must be stated here, however, that the different inverse lifetimes can only be obtained if the group exchange processes modulate the spin hamiltonian of the A and/or of the isotopes L and M. For this purpose, suitable spin labels have to be introduced into the A residue. The above kinetic quantities are sufficient to describe the NMR lineshapes. Thus, it is not necessary to make assumptions on reaction mechanisms during the state of the analysis of the spectra. As shown in the following, information on the reactions present can then be obtained from the dependence of these quantities on the deuterium content of the sample.

In order to illustrate the rationale behind this procedure we will present some examples of how to relate the above inverse lifetimes to specific mechanisms of hydrogen/deuterium exchange.

3.1.1. Single Intermolecular Hydrogen Transfer Reactions

Let us consider a catalyzed single proton transfer mechanism of the type

$$\begin{aligned}
&\mathrm{AH} + \mathrm{A^*}^- \xrightarrow{k_1^{\mathrm{H}}} \mathrm{A}^- + \mathrm{A^*H},\\
&\mathrm{A}^- + \mathrm{A^*D} \xrightarrow{k_1^{\mathrm{D}}} \mathrm{AD} + \mathrm{A^*}^-, \qquad (10)
\end{aligned}$$

where k_1^{L} corresponds to a second order constant. Assuming that A^- is present only in a very low concentration, it follows from conventional kinetics that

$$\tau^{-1}_{\mathbf{AHA^*H}} = \tau^{-1}_{\mathbf{AHAH^*}} = \tau^{-1}_{\mathrm{AH}} = k_1^{\mathrm{H}}\, C_{\mathrm{A}^-}, \qquad (11)$$

$$\tau^{-1}_{\mathbf{ADA^*D}} = \tau^{-1}_{\mathbf{ADAD^*}} = \tau^{-1}_{\mathrm{AD}} = k_1^{\mathrm{D}}\, C_{\mathrm{A}^-}, \qquad (12)$$

$$\tau^{-1}_{\mathbf{AHAD}} = k_1^{\mathrm{H}}\, k_1^{\mathrm{D}}/(k_1^{\mathrm{H}} + k_1^{\mathrm{D}})\, C_{\mathrm{A}^-}. \qquad (13)$$

Thus, the different inverse lifetimes are independent of the deuterium fraction in the mobile proton sites. Sometimes it is convenient to incorporate the total concentration C_{A} into the rate constants k_1^{L} which then become pseudo first order rate constants.

3.1.2. Double Intermolecular Hydrogen Transfer Reactions

Let us first consider the basic hydrogen exchange reaction between two different labile protons sites AH and XH, i.e., the following isotopic double hydrogen transfer reaction set:

$$\mathrm{AH} + \mathrm{A^*H^*} \xrightarrow{k_2^{\mathrm{HH}}} \mathrm{AH^*} + \mathrm{A^*H}, \qquad (14)$$

$$\mathrm{AH} + \mathrm{A^*D} \xrightarrow{k_2^{\mathrm{HD}}} \mathrm{AD} + \mathrm{A^*H}, \qquad (15)$$

$$\mathrm{AD} + \mathrm{A^*D^*} \xrightarrow{k_2^{\mathrm{DD}}} \mathrm{AD^*} + \mathrm{A^*D}. \qquad (16)$$

Let k_2^{LM} be the pseudo second order rate constants of the different forward isotopic reactions whose rate constants are to be determined. In contrast to single proton transfer reactions, the above inverse group lifetimes depend on the deuterium fractions D in the mobile proton site AL. By measuring these lifetimes as a function of D, the three independent isotopic rate constants k^{HH}, k^{HD}, k^{DH} and k^{DD} can easily be derived. Let

$$C_{\mathrm{A}} = C_{\mathrm{AH}} + C_{\mathrm{AD}} \qquad (17)$$

be the total concentration of A. Using conventional kinetics we obtain

$$\tau^{-1}_{\mathbf{AHAH^*}} = k_2^{\mathrm{HH}}\, C_{\mathrm{AH}} = (1-D)\, k_2^{\mathrm{HH}}\, C_{\mathrm{A}}, \qquad (18)$$

$$\tau^{-1}_{\mathbf{AHAD}} = k_2^{\mathrm{HD}}\, C_{\mathrm{AD}} = D\, k_2^{\mathrm{HD}}\, C_{\mathrm{A}}, \qquad (19)$$

$$\tau^{-1}_{\mathbf{ADAH}} = k_2^{\mathrm{HD}}\, C_{\mathrm{AH}} = (1-D)\, k_2^{\mathrm{HD}}\, C_{\mathrm{A}}, \qquad (20)$$

$$\tau^{-1}_{\mathbf{ADAD^*}} = k_2^{\mathrm{DD}}\, C_{\mathrm{AD}} = D\, k_2^{\mathrm{DD}}\, C_{\mathrm{A}}, \qquad (21)$$

$$\begin{aligned}
\tau^{-1}_{\mathbf{AHXH}} &= \tau^{-1}_{\mathrm{AH}} = k_2^{\mathrm{HH}}\, C_{\mathrm{AH}} + k_2^{\mathrm{HD}}\, C_{\mathrm{AD}}\\
&= ((1-D)\, k_2^{\mathrm{HH}} + D\, k_2^{\mathrm{HD}})\, C_{\mathrm{A}}, \qquad (22)\\
\tau^{-1}_{\mathbf{ADXD}} &= \tau^{-1}_{\mathrm{AD}} = k_2^{\mathrm{HD}}\, C_{\mathrm{AH}} + k_2^{\mathrm{DD}}\, C_{\mathrm{AD}}\\
&= ((1-D)\, k_2^{\mathrm{HD}} + D\, k_2^{\mathrm{DD}})\, C_{\mathrm{A}}. \qquad (23)
\end{aligned}$$

All quantities are linearly dependent on the deuterium fraction D. Again, it is sometimes convenient to incor-

porate the total concentration C_A into the rate constants k_2^{LM}, which then become pseudo first order rate constants.

3.1.3. Triple Intermolecular Hydrogen Transfer Reactions

For a triple hydrogen transfer self exchange reaction one has to consider the following isotopic reactions

$$AH + A^*H^* + A'H' \xrightarrow{k_3^{HHH}} AH^* + A^*H' + A'H, \quad (24)$$

$$AH + A^*H^* + A'D \xrightarrow{k_3^{HHD}} AH^* + A^*D + A'H, \quad (25)$$

$$AH + A^*D + A'D' \xrightarrow{k_3^{HDD}} AD + A^*D' + A'H, \quad (26)$$

$$AD + A^*D^* + A'D' \xrightarrow{k_3^{DDD}} AD^* + A^*D' + A'D. \quad (27)$$

In a similar way to that in the previous section we then obtain

$$\tau_{\mathbf{AHAH^*}}^{-1} = k_3^{HHH} C_{AH}^2 + k_3^{HHD} C_{AH} C_{AD}$$
$$= [(1-D)^2 k_3^{HHH} + (1-D) D k_3^{HHD}] C_A^2, \quad (28)$$

$$\tau_{\mathbf{AHAD}}^{-1} = k_3^{HHD} C_{AH} C_{AD} + k_3^{HDD} C_{AD}^2$$
$$= [D(1-D) k_3^{HHD} + D^2 k_3^{HDD}] C_A^2, \quad (29)$$

$$\tau_{\mathbf{ADAH}}^{-1} = k_3^{HHD} C_{AH} C_{AD} + k_3^{HDD} C_{AD}^2$$
$$= [D(1-D) k_3^{HDD} + (1-D^2) k_3^{HHD}] C_A^2, \quad (30)$$

$$\tau_{\mathbf{ADAD^*}}^{-1} = k_3^{HDD} C_{AH} C_{AD} + k_3^{DDD} C_{AD}^2$$
$$= [D(1-D) k_3^{HDD} + D^2 k_3^{DDD}] C_A^2, \quad (31)$$

$$\tau_{\mathbf{AHXH}}^{-1} = \tau_{AH}^{-1} = k_3^{HHH} C_{AH}^2 + 2 k_3^{HHD} C_{AH} C_{AD} + k_3^{HDD} C_{AD}^2$$
$$= [(1-D)^2 k_3^{HHH} + 2(1-D) D k_3^{HHD} + D^2 k_3^{HDD}] C_A^2, \quad (32)$$

$$\tau_{\mathbf{ADXD}}^{-1} = \tau_{AD}^{-1} = k_3^{HHD} C_{AH}^2 + 2 k_3^{HDD} C_{AH} C_{AD} + k_3^{DDD} C_{AD}^2$$
$$= [(1-D)^2 k_3^{HHD} + 2 D(1-D) k_3^{HDD} + D^2 k_3^{DDD}] C_A^2. \quad (33)$$

Now, the inverse average lifetimes are quadratically dependent on the deuterium fraction D. Again, it is convenient now to incorporate the term C_A^2 into the third order rate constants, which then become pseudo first order rate constants.

3.1.4. Superposed Double and Triple and Other Multiple Proton Transfer

By comparing (18)–(23) with (28)–(33) it should be immediately apparent that the inverse lifetimes measured are independent of the particular reaction scheme. Thus, a superposed double and triple proton transfer reaction can be described just by adding up the corresponding equations. The nature of the reaction scheme of interest is most easily determined at fixed concentrations of the reactants as a function of the deuterium fraction of the sample. The treatment of multiple proton transfer reactions with $n>3$ is, in principle, straightforward. However, as the number of measurable different lifetimes is constant and the number of rate constants to be determined drastically increases, the analysis of experimental data will become difficult.

3.2. NMR Lineshape Theory

We assume a general understanding of the theory of exchange broadened NMR lineshapes and will restrict ourselves to particular equations necessary for an understanding of how the dynamic quantities defined in the previous section can be obtained by lineshape analysis. It has been shown [22, 54–57] that all the information on NMR lineshapes is contained in a complex matrix $\mathcal{M}$ and a population vector $\boldsymbol{P}$ calculated according to quantum mechanical density matrix theory. The dimension of $\mathcal{M}$ corresponds to the number of NMR transitions which have to be considered in the regime of slow exchange. The imaginary part of the eigenvalues of $\mathcal{M}$ corresponds to the position of the NMR lines, the real part to their width. From the eigenvectors of $\mathcal{M}$ and the population vector a complex intensity vector can be constructed. The real part of this vector describes the intensity of the Lorentzian and the imaginary part the intensity of a dispersion line associated to a given transition. When the spin systems are of first order, $\mathcal{M}$ and $\boldsymbol{P}$ can be set up by inspection, using the simpler Kubo-Sack theory [54] based on the modified Bloch equations. In all cases one has to keep in mind that the Larmor frequency of the nuclei studied must be modulated by the exchange process to be monitored.

3.2.1. ^{1}H NMR of an AH Spin System in the Presence of Intermolecular Proton Exchange

As an example relevant in the context of this study, let us consider a spin system AH, where A represents a spin 1/2 nucleus, in the presence of intermolecular proton exchange. Let the difference between the Larmor frequencies ν_A of A and ν_H of the exchanging proton be such that AH constitutes a first order spin

system. Further, let us analyze only the lineshape of the exchanging proton affected, as described in the previous section, by the inverse lifetime $\tau^{-1}_{\mathbf{AHA^*H}} \equiv \tau^{-1}_{\mathbf{AH}}$. The complex exchange matrix $\mathscr{M}$ and the population vector are then given by

$$\mathscr{M} = \begin{pmatrix} -\tau^{-1}_{\mathbf{AHA^*H}}/2 - \pi W_0 + 2\pi i(\nu_H + J_{AH}/2) & \tau^{-1}_{\mathbf{AHA^*H}}/2 \\ \tau^{-1}_{\mathbf{AHA^*H}}/2 & -\tau^{-1}_{\mathbf{AHA^*H}}/2 - \pi W_0 + 2\pi i(\nu_H - J_{AH}/2) \end{pmatrix}, \quad \boldsymbol{P} = \begin{pmatrix} 1/2 \\ 1/2 \end{pmatrix}. \tag{34}$$

In the slow exchange range the signal of the exchanging proton consists of a doublet at the frequency ν_A with a splitting corresponding to the coupling constant J_{AH}. The two line components refer to the protons attached to nuclei A in the spin states α(A) and β(A). When the proton exchanges, its Larmor frequency is modulated from $\nu_A + J_{AH}$ to $\nu_A - J_{AH}$. This switch occurs, however, only every other exchange process. Thus, the inverse lifetimes are divided by 2 in (34). As the proton transfer speeds up, the two lines broaden and coalesce into one single line at the position ν_A. Note that in (34) no assumptions concerning the proton exchange mechanism have been made. Information on the mechanism can be obtained by performing experiments at different deuterium fractions D, as described in section 4.

3.2.2. NMR Lineshape Theory of Remote Spins in Proton Donors in the Presence of Intermolecular Proton Exchange

By studying remote spins A in proton donors of the type AL, L = H, D, the isotopic selectivity encountered in the study of L spins is lost. Thus, both species AH and AD contribute to the lineshape of A. Let us consider here the simplest case, where scalar coupling between A spins and L spins can be neglected. In this case the NMR lineshape of A is sensitive to the proton exchange only when the chemical shift of A is modulated by the exchange. Let ν_{AL} be the chemical shift of A before and $\nu_{A'L}$ the chemical shift after the exchange. We obtain the following exchange and population vector:

$$\boldsymbol{P} = [p_{AH}, p_{AH}, p_{AD}, p_{AD}], \quad \tau^{-1}_{\mathbf{AHAD}}/\tau^{-1}_{\mathbf{ADAH}} = p_{AD}p_{AH}. \tag{35}$$

Generally, $p_{AH} = (1 - D)$ and $p_{AD} = D$.

An experimental example where these equations apply will be given below.

$$\mathscr{M} = \begin{pmatrix} -\tau^{-1}_{\mathbf{AHAH^*}} - \pi W_0 & -\tau^{-1}_{\mathbf{AHAD}} + 2\pi i \nu_{AH} & \tau^{-1}_{\mathbf{AHAH^*}} & & & \tau^{-1}_{\mathbf{ADAH}} \\ \tau^{-1}_{\mathbf{AHAH^*}} & -\tau^{-1}_{\mathbf{AHA'H^*}} - \pi W_0 & -\tau^{-1}_{\mathbf{AHAD}} + 2\pi i \nu_{A'H} & \tau^{-1}_{\mathbf{ADAH}} & & \\ & \tau^{-1}_{\mathbf{AHAD}} & -\tau^{-1}_{\mathbf{ADAH}} - \pi W_0 & -\tau^{-1}_{\mathbf{ADAD}} + 2\pi i \nu_{AD} & \tau^{-1}_{\mathbf{ADAD^*}} & \\ & \tau^{-1}_{\mathbf{AHAD}} & & \tau^{-1}_{\mathbf{ADAD^*}} & -\tau^{-1}_{\mathbf{ADAH}} - \pi W_0 & -\tau^{-1}_{\mathbf{ADAD}} + 2\pi i \nu_{A'D} \end{pmatrix}$$

4. Results

In these section, the essential features of the theory developed above are applied to the problem of determinating the number m of protons transferred in the rate limiting step of proton self exchange of DFFA (Figs. 1 and 2) dissolved in THF, as well as the associated multiple kinetic isotope effects.

4.1. ^1H 300.13 MHz NMR Spectra of DFFA as a Function of the Deuterium Fraction D in the Mobile Proton Sites

In order to determine m we have measured the ^1H 300.13 MHz NMR spectra of DFFA as a function of the deuterium fraction D in the mobile proton sites at a temperature of 189.2 K and a total DFFA concentration of $C_{298\,K} = 0.02$ mol l^{-1}. As DFFA was labeled with ^{15}N, the signal of the labile proton should split into a ^1H–^{15}N doublet in the absence of intermolecular proton exchange. By contrast, fast proton exchange should modulate the Larmor frequency of the mobile proton from $\nu_a + J_{ab}$ to $\nu_a - J_{ab}$ every other exchange process, which eventually leads to a collapse of the doublet into a singlet, as predicted by (34). ν_a is the chemical shift of the mobile proton and J_{ab} the ^1H–^{15}N coupling constant.

The superposed experimental and simulated ^1H–^{15}N signals of DFFA in THF are shown in Figure 3. Two signals are observed. Whereas signal A_a is associated

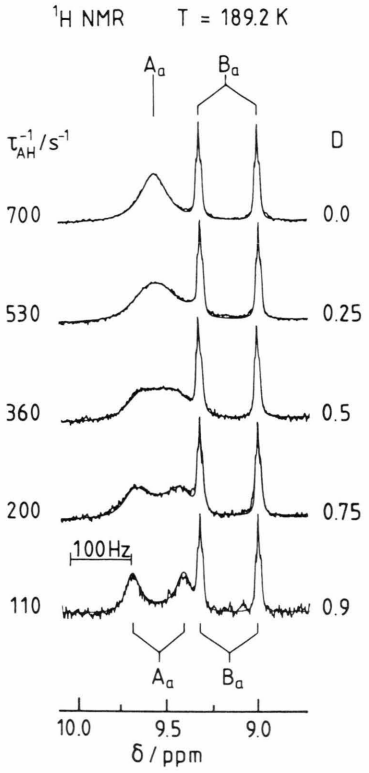

Fig. 3. Superposed experimental and calculated 300.13 MHz $^1H-^{15}N$ NMR signals of 0.02 molar solutions of DFFA at 189.2 K as a function of the deuterium fraction D in the $^1H-^{15}N$ position. The $^1H-^{15}N$ signals of the s-trans form A are labeled as A_a and of the s-cis form B as B_a in accordance with Fig. 2. The inverse proton lifetimes in X=A, B are labeled as τ_{XH}^{-1}. τ_{BH}^{-1} was set to zero.

with the s-trans form A, signal B_a can be assigned to the s-cis form B (for atom numbering see Figure 2). Signal B_a does not show any signs of exchange broadening due to proton transfer, i.e. it consists of a sharp $^1H-^{15}N$ doublet at all values of the deuterium fraction D; both doublet components are further split into triplets by coupling with the CH atom c and the second ^{15}N atom d. Thus, conformer B is not able to exchange protons, in contrast to conformer A. The $^1H-^{15}N$ signal of the latter evolves from an exchange broadened singlet at $D=0$ to an exchange broadened doublet at $D=0.9$. This observation signifies that the proton exchange between A molecules is already fast at $D=0$ but slows down when the deuterium fraction is increased. Therefore, the lifetime $\tau_{AHA^*H} \equiv \tau_{AH}$ of a proton in a given molecule AH before the jump to a chemically equivalent but physically different group A* depends on whether the other molecules are proto-

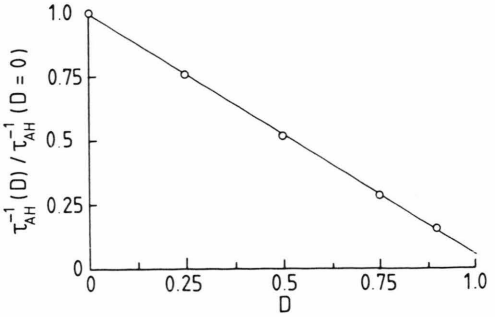

Fig. 4. ^{1}H NMR proton inventory plot of the data in Fig. 2. In accordance with (22), a linear dependence $\tau_{AH}^{-1} = f(D)$ is expected for a double proton transfer process. The ratio $\tau_{AH}^{-1}(D=0)/\tau_{AH}^{-1}(D=0)$ represents the kinetic HH/HD isotope effect of the exchange.

nated or deuterated. This is the first indication that A is involved in a multiple proton transfer process. Note that the chemical shifts of signal A_a are extremely dependent on temperature and concentration. The fact that the signal positions in Fig. 2 are constant within the margin of error indicates that both temperature and concentration constancy has been achieved in the set of spectra in Figure 3.

4.2. ^1H NMR Lineshape Analysis of the $^1H-^{15}N$ Signal of DFFA in THF

To simulate the spectra in Fig. 3 we followed the procedures recently described for the non-fluorinated compound [31]. Only the inverse proton lifetimes τ_{AH}^{-1} needed to be varied. The linewidths W_0 in the absence of exchange were determined by lineshape analysis of the signal B_a. As previously [31], we did not use (34) to calculate the spectra but a slightly more complicated equation which takes into account the additional couplings to the CH proton and the second ^{15}N nucleus. The following values were used for the simulation of the spectra in Figure 3: $J_{A_{ab}} = J_{B_{ab}} = 91.8$ Hz, $J_{A_{ac}} \cong 9.8$ Hz, $J_{A_{ad}} \cong 3.0$ Hz, $J_{B_{ac}} \cong J_{B_{ad}} \cong 4.2$ Hz. In addition, the chemical shifts $\delta_{A_a} = 9.55$ ppm and $\delta_{B_a} = 9.15$ ppm were employed. Finally, the A/B ratio was calculated as $I = C_A/C_B = 1.4$.

4.3. ^1H NMR Proton Inventory

In Fig. 4 we have plotted the ratio of the inverse proton lifetimes in $A \equiv AH$, $\tau_{AHA^*H}^{-1}(D)/\tau_{AHA^*H}^{-1}(D=0) \equiv \tau_{AH}^{-1}(D)/\tau_{AH}^{-1}(D=0)$ as a function of D. We observe a

nicely linear decrease, as predicted by (22) for a double proton transfer process with $m=2$. The inverse lifetimes $\tau_{\mathbf{AH}}^{-1}(D=0)$ and $\tau_{\mathbf{AH}}^{-1}(D=1)$ can then be identified as the pseudo first order rate constants k_2^{HH} and k_2^{HD} of the processes

$$\mathrm{AH}+\mathrm{A^*H^*} \xrightarrow{k_2^{HH}} \mathrm{AH^*}+\mathrm{A^*H},$$
$$\mathrm{AH}+\mathrm{A^*D} \xrightarrow{k_2^{HD}} \mathrm{AD}+\mathrm{A^*H}.$$

By linear regression analysis we obtain $k_2^{HH}=700\pm20\ \mathrm{s}^{-1}$ and $k_2^{HD}=37\pm5\ \mathrm{s}^{-1}$, i.e. a kinetic HH/HD isotope effect of $k_2^{HH}/k_2^{HD}=19\pm3$. The relative large error of the latter quantity is explained by the fact that we were not able to measure τ_{AH} values at $D>0.9$ in this study.

4.4. ^{19}F NMR Spectra of DFFA as a Function of the Deuterium Fraction D in the Mobile Proton Sites

Using the information that $m=2$, we were able to obtain the full kinetic HH/HD/DD isotope effects by dynamic ^{19}F NMR measurements at 84.7 MHz. Figure 5 shows the superposed experimental and calculated ^{19}F NMR spectra of DFFA at 189.2 K and a concentration of $C_{298\,K}=0.02\ \mathrm{mol\,l}^{-1}$ as a function of the deuterium fraction D. The spectra in Fig. 5 were obtained from the same samples whose ^1H NMR signals are shown in Fig. 3, with the exception of the highest deuterated sample ($D=0.99$). All spectra were taken under exactly the same experimental conditions, each with a total number of 1500 scans.

One major difference between the spectra in Figs. 3 and 5 is that in Fig. 3 only the protonated molecules AH and BH are observed, whereas in Fig. 5 both $A=\{AH, AD\}$ and $B=\{BH, BD\}$ contribute to the spectra. Two singlets $B_e=\{BH_e, BD_e\}$ and $B_f=\{BH_f, BD_f\}$ (see atom numbering in Fig. 2) are observed for the s-cis form B, indicating two inequivalent fluorine atom positions in this species, which is conform with the molecular structure. Again, the signals B_e and B_f do not depend on D. By contrast, the lineshape of the fluorine signals of A strongly depends on the deuterium fraction D. Let us first take a look at the spectrum with $D=0.99$. Two sharp signals AD_e and AD_f are observed, which indicate two inequivalent fluorine positions in the AD molecule, as expected for a slow deuterium exchange. Now, at $D=0$ one broadened coalesced fluorine signal $AH_{e,f}\equiv AH_e, AH_f$ is observed, indicating that a fast process takes place between protonated AH molecules, rendering the two

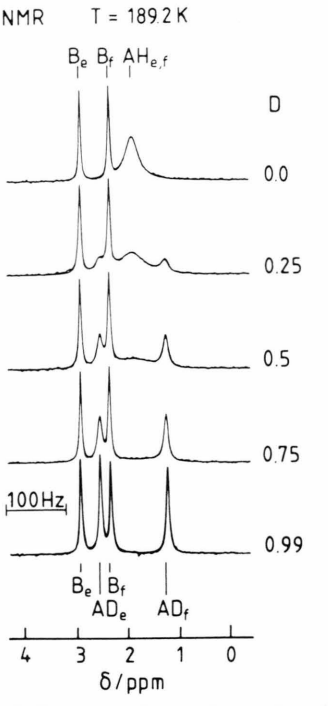

Fig. 5. Superposed experimental and calculated ^{19}F-{^1H}-NMR spectra of 0.02 molar solutions of DFFA in THF as a function of the deuterium fraction D. For the explanation of the atom labeling see Figure 2. The pseudo first order rate constants of the proton exchange are labeled as k_2^{LM}, LM = HH, HD, DD. In the fitting procedure, k_2^{DD} was set constant to a value of $3\ \mathrm{s}^{-1}$ (see Figs. 6 and 7); by simultaneous non-linear regression analysis of all spectra we obtained $k_2^{HH}=700\ \mathrm{s}^{-1}$ and $k_2^{HD}=33\ \mathrm{s}^{-1}$. The linewidth in the absence of exchange $W_0\approx5$ Hz was obtained from the B_e and B_f signals.

inequivalent AH_e and AH_f fluorine atoms equivalent. In view of the molecular structure of DFFA and the dependence of this process on the deuterium fraction, it must correspond to the intermolecular double proton transfer described for ^1H in the previous section. It involves two AH molecules of the type shown in Fig. 1, where the proton exchange is associated with an intramolecular exchange of ^{19}F atoms.

Now, a very interesting novel phenomenon is observed at intermediate deuterium fractions: the fluorine atoms of the protonated AH and the deuterated AD molecules can be separated, giving rise to a line trio. Whereas the outer two singlets of the trio stem from the AD_e and AD_f, the inner broad line stems from the coalesced AH_e, AH_f fluorine atoms. As D increases, the latter signal becomes broader indicating longer lifetimes of the mobile proton in AH. By contrast, the deuteron lifetime in the deuterated AD

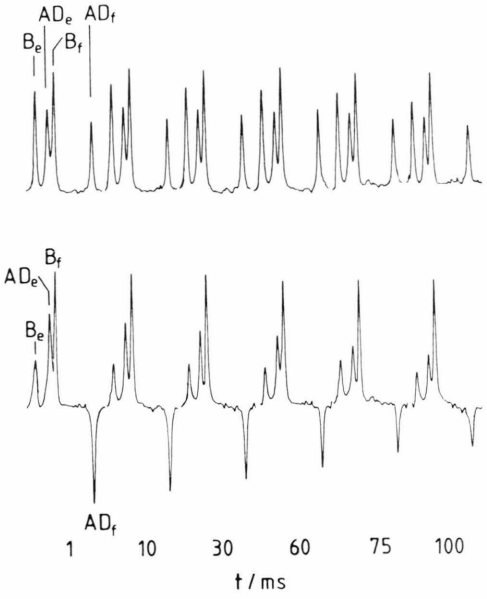

Fig. 6. ^{19}F-magnetization transfer experiments in the rotating frame of a 0.02 molar solution of DFFA in THF at a deuterium fraction of $D=0.99$ in the mobile proton sites. The carrier frequency was set to the position of the AD_f line. Upper curves: experiment (i), corresponding to a usual $T_{1\varrho}$ experiment; lower curve: experiment (ii) with a delay $\tau=1/(2\Delta\nu)=4.2$ ms between the first 90° pulse and the spin locking pulse. $\Delta\nu$ is the frequency difference between the signals AD_e and AD_f. B_e, B_f: non exchanging, AD_e, AD_f: exchanging magnetizations. Repetition time 3.8 s, 4.2 μs 90° pulses, strength of the spin locking field $t_{180°}=165$ μs.

molecules shortens as D decreases, leading to a broadening of the outer two singlets. Note that the line intensities AH_e and AH_f are given by $C_A(1-D)/2$ whereas the line intensities AD_e and AD_f are given by $C_A D/2$.

4.5. ^{19}F NMR Lineshape Analysis and Magnetization Transfer of DFFA in THF

The spectra in Fig. 5 were analyzed using the exchange matrix of (35). Unfortunately, not all kinetic quantities $\tau^{-1}_{\mathbf{AHAH^*}}(D)$, $\tau^{-1}_{\mathbf{AHAD}}(D)$, $\tau^{-1}_{\mathbf{AHAD}}(D)$, and $\tau^{-1}_{\mathbf{ADAD^*}}(D)$ could be obtained for all values of D. This is obvious because AD does not contribute to the lineshape at $D=0$. The same is true for AH at $D=1$. Therefore, it was a great help to know from the ^{1}H spectra that $m=2$, i.e. that (18)–(22) apply and these deuterium fraction dependent quantities could be replaced by the three pseudo first order rate constants k_2^{HH}, k_2^{HD}, and k_2^{DD} in the following way:

$$\tau^{-1}_{\mathbf{AHAH^*}}=(1-D)\cdot k_2^{HH},\quad \tau^{-1}_{\mathbf{AHAD}}=D\cdot k_2^{HD}, \tag{36}$$

$$\tau^{-1}_{\mathbf{ADAH}}=(1-D)\cdot k_2^{DH},\quad \tau^{-1}_{\mathbf{ADAD^*}}=D\cdot k_2^{DD}. \tag{37}$$

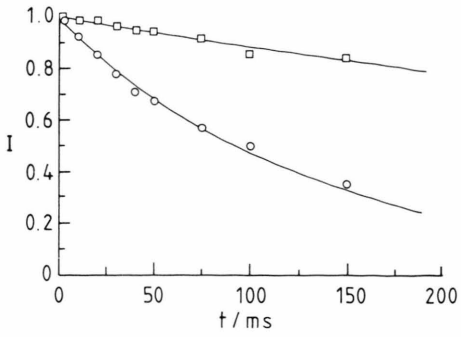

Fig. 7. Analysis of the data in Figure 6. Parameters of the non-linear regression analysis: $T_{1\varrho}=808$ ms and $k_2^{DD}=3.05\ s^{-1}$.

The value of k_2^{HH} was determined from the spectrum at $D=0$; this value coincides nicely with the corresponding value obtained by ^{1}H NMR lineshape analysis. Unfortunately, the value of $k_2^{DD}=3\ s^{-1}$ was too small to induce a measurable line broadening. The latter value was, therefore, determined by the method of "magnetization transfer in the rotating frame" [27] between the lines AD_e and AD_f at $D=0.99$, as shown below. From the spectra in the intermediate D range then we obtained values of $k_2^{HD}=33\ s^{-1}$ by non-linear least squares fitting of the simulated to the experimental spectra. Again, W_0 was determined by simulation of the signals B_e and B_f.

The results of the magnetization transfer experiments are shown in Figs. 6 and 7. For this purpose two sets of experiments were carried out. In the "parallel" experiment (i) the decay of the magnetizations AD_e and AD_f is governed solely by the longitudinal relaxation time in the rotating frame, $T_{1\varrho}$ [27]:

$$M_{AD_f}=M_{AD_f}(t=0)\exp(-t/T_{1\varrho}), \tag{38}$$

whereas in the "antiparallel" experiment (ii)

$$M_{AD_f}=M_{AD_f}(t=0)\exp(-t(2k_2^{DD}+T_{1\varrho}^{-1})). \tag{39}$$

Since it was difficult to measure the line intensity of AD_e because of signal overlap, only the integrated intensities of AD_f were used to determine k_2^{DD} by non-linear-least-squares fitting of the data shown in Figure 7.

We obtained the following kinetic isotope effects at 189.2 K and a concentration of $C_{298\,K}=0.02\ mol\ l^{-1}$:

$$k_2^{HH}/k_2^{DD}=233\pm20,\quad k_2^{HH}/k_2^{HD}=21\pm3 \text{ and}$$

$$k_2^{HD}/k_2^{DD}=\ 11\pm\ 2.$$

These k_2^{HH}/k_2^{HD} values are in good agreement with those obtained in the ^{1}H NMR experiments.

5. Discussion

We have described a strategy to measure the number m of protons transferred in a proton self exchange reaction as well as the associated multiple kinetic isotope effects by a combination of different NMR proton inventories of exchanging hydrogen isotopes or of remote spins such as ^{19}F, ^{13}C, ^{15}N, or ^{1}H atoms that are not in flight in the rate limiting reaction step. In such proton inventories, kinetic quantities are measured as a function of the deuterium fraction D in the mobile proton sites. As an example, we have performed dynamic ^{1}H and ^{19}F NMR experiments on the proton exchange of DFFA (Figs. 1 and 2) dissolved in THF. Since the proton exchange process averages out the scalar $^{1}H-^{15}N$ coupling constant as well as the ^{19}F chemical shifts in the two different aryl rings of DFFA, proton exchange rates could be determined by ^{1}H and ^{19}F lineshape analysis and magnetization transfer measurements. A linear decrease of the proton exchange rates detected by ^{1}H NMR with the deuterium fraction in the mobile $^{1}H-^{15}N$ site of DFFA showed that $m=2$ protons are transferred in the rate limiting step of the reaction. The full kinetic HH/HD/DD isotope effects could then be obtained from the NMR experiments on the remote ^{19}F spins. We find a kinetic HH/DD isotope effect of 233 at 189.2 K. To our knowledge this is the largest kinetic hydrogen/deuterium isotope effect established so far by dynamic NMR spectroscopy. We further find the partial kinetic HH/HD and HD/DD isotope effects of 21 and 11. The rule of the geometric mean (RGM) would predict for both partial quantities equal values of 15.

In the remainder of this discussion we try to relate these results to the mechanism of the proton exchange process in DFFA. First, let us recall different possibilities to explain large deviations from the RGM. For the case of a stepwise proton transfer process a large deviation is expected as only one proton is transferred in the rate limiting step [17–19, 33]. Whereas the transferred proton leads to a single primary kinetic isotope effect P, the second proton merely induces a secondary kinetic isotope effect S. For a reaction along a symmetric triple minimum potential the following relations were derived without any assumptions about an over barrier or a tunneling pathway [33]:

$$\frac{k^{HD}}{k^{DD}} = \frac{2}{S^{-1}+P^{-1}} \quad \text{and} \quad \frac{k^{HH}}{k^{DD}} = P \cdot S. \qquad (40)$$

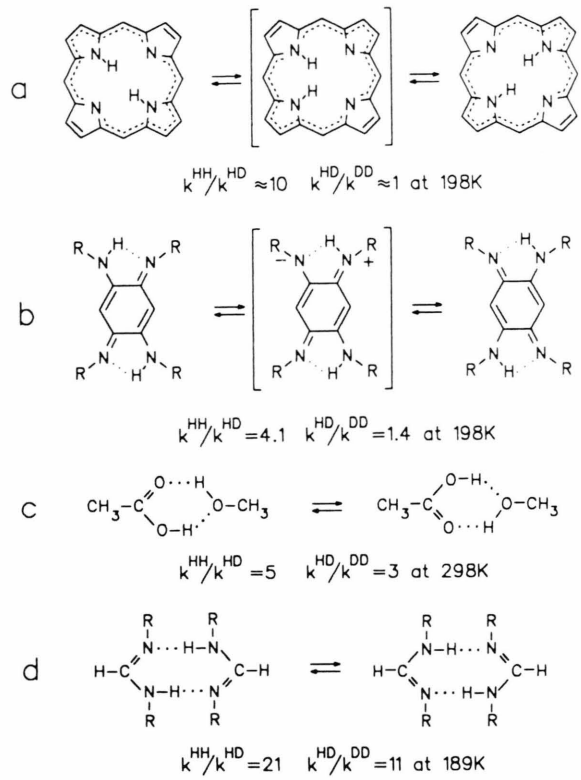

Fig. 8. Comparison of kinetic HH/HD/DD isotope effects of differential intra- and intermolecular double proton transfer reactions. a) Porphyrine [17], b) azophenine [32], c) acetic acid/methanol [21], d) DFFA (this study). The species in square brackets are postulated intermediates.

Since S is of the order of 1 and $P \gg 1$ it follows that $k^{HH}/k^{DD} \approx P$ and $k^{HD}/k^{DD} \approx 2$, which signifies a very large deviation from the RGM. In the case of a concerted double proton transfer reaction, deviations from the RGM are very small when the reaction proceeds over the barrier [16–19], but can be substantial when tunneling is involved [17–21].

In order to interpret the DFFA results it is helpful to make a comparison with other inter- and intramolecular proton transfer systems shown in Fig. 8 for which full kinetic isotope effects have been observed previously. The deviation from the RGM is very large in the case of the intramolecular tautomerism of porphine [17] and of azophenine [32]. In the case of azophenine the kinetic data were consistent with a reaction over the barrier, and the kinetic isotope effects were interpreted in terms of (40) with values of $P_{298\,K}=7.2$, $S_{298\,K}=0.78$ at 298 K. Novel independent

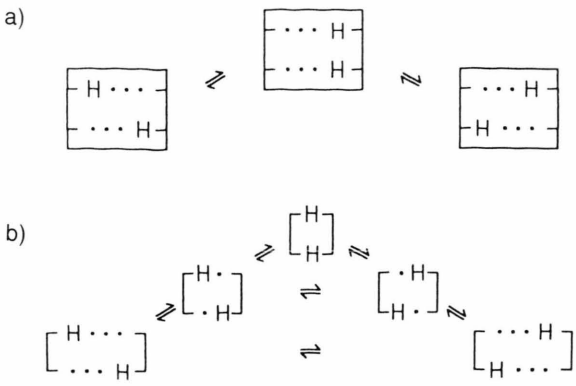

Fig. 9. a) Stepwise double proton transfer in the case of a fixed molecular frame of heavy atoms. b) Double proton transfer in the case of variable hydrogen bond lengths according to a model proposed in [21]. For further explanation see text.

theoretical and experimental studies also favor a stepwise mechanism for the tautomerism of porphyrine [34], i.e. an interpretation of the kinetic HH/HD/DD isotope effects in terms of (40). The large isotope effects still favor a tunnel mechanism of this reaction.

Equation (40) is, however, not able to accomodate either the acetic acid/methanol or the DFFA data. This would involve a primary kinetic single hydrogen/deuterium isotope effect of $P=36$ and a secondary effect of $S=6.5$ for DFFA at 189.2 K. It is clear that such data exceed the range of values for secondary kinetic isotope effects [4]. Thus, the DFFA results as well as those of acetic acid/methanol apparently support a concerted transfer mechanism in these compounds.

We try now to give a qualitative explanation for the different behavior of the different double proton transfer systems. This explanation is based on the observation that porphyrine [25] and azophenine [32] lack the usual flexibility of hydrogen bonded systems, i.e. the usual low frequency hydrogen bond stretching vibration [3] that modulates the hydrogen bond distance. Thus, the molecular frame of heavy atoms in these compounds is relatively rigid, and a high energy would be required to reduce the hydrogen bond distance in such systems. This feature is expressed in Fig. 9a by an outer square, which schematically represents the molecular frame. It is understandable that it costs too much energy to break the bonds of both protons to their neighboring heavy atoms at the same time, and the proton transfer will be asynchronous [58]. Note that proton tunneling in this case will always require a minimum energy of activation corresponding to the energy difference between the intermediate and the initial state [59].

By contrast, the presence of low frequency hydrogen bond stretching vibrations in the flexible intermolecular proton transfer systems allows a comparatively easy compression of the hydrogen bond, as schematically shown in the model of Figure 9b. This model has been already proposed to describe the proton transfer between acetic acid and methanol [17, 21]. In this case the hydrogen bond lengths are variable, i.e. the energy of activation of the proton transfer is pooled into the hydrogen bond stretching vibration which shortens the hydrogen bond length. A consequence of the shorter bond length is a smaller barrier to the proton transfer which might be stepwise or concerted. At extremely short hydrogen bond lengths the barrier to proton transfer and, therefore, the difference between a stepwise and a concerted proton transfer mechanism vanishes. The imaginary frequency required for a transition state then corresponds to the hydrogen bond stretching rather than to the AH-stretching vibrations. However, it is well known that the latter are shifted to lower frequencies when the hydrogen bond distance is shortened [60]. Therefore, there will be a considerable loss of zero point energy in both vibrations in the highly compressed transition state, and the RGM will be fulfilled at high temperatures. At lower temperatures the transfer may occur by tunneling, leading to violation of the RGM at low temperatures, as has been discussed previously [17, 21]. Thus, for the intermolecular proton transfer systems of Fig. 8 we propose a reaction mechanism according to Figure 9b. However, further kinetic studies, especially the determination of the kinetic HH/HD/DD isotope effects of the DFFA reaction as a function of temperature, as well as of further proton transfer systems is necessary in order to substantiate this evidence. Note that one might find intermolecular proton transfer systems with rigid hydrogen bond distances and intramolecular proton transfer systems with flexible hydrogen bonds, which could lead to an inversed behavior of kinetic isotope effects.

6. Conclusions

We conclude that it is possible to study multiple kinetic isotope effects of proton self exchange reactions by NMR spectroscopy as long as the molecules

studied contain spin labels whose chemical shifts are modulated by the exchange process. Of additional help are scalar spin–spin couplings of protons to the heavy atoms which they are bounded , e.g. ^{15}N atoms. In the future one might also use dipolar or quadrupolar interactions of protons or deuterons for the study of proton exchange reactions when anisotropic media such as liquid crystals are used as solvents. In addition to reactions in liquids, kinetic isotope effect studies of proton transfer processes in solids, for which some examples have already been given [35, 43], might also be fruitful. The results presented in this study have shown that NMR studies of multiple kinetic isotope effects might be useful for the further development of the theory of kinetic isotope effects which has been initiated by Professor R. P. Bell and by Professor Jacob Bigeleisen to whom this paper is dedicated at the occasion of his 70th birthday.

Acknowledgements

We thank the Deutsche Forschungsgemeinschaft, Bonn-Bad Godesberg and the Fonds der Chemischen Industrie Frankfurt for financial support. The calculations were done on the Univac 1108 computer of the Rechenzentrum der Universität Freiburg i. Br.

[1] R. P. Bell, The Tunnel Effect in Chemistry, Chapman and Hall, London 1980.
[2] R. D. Gandour and R. L. Schowen, Transition States of Biochemical Processes, Plenum Press, New York 1978.
[3] The Hydrogen Bond (P. Schuster, G. Zundel, and C. Sandorfy, eds.), North-Holland Publ. Comp., Amsterdam 1976.
[4] L. Melander and W. H. Sauders, Reaction Rates of Isotopic Molecules, John Wiley & Sons, New York, Toronto 1980.
[5] C. G. Swain and J. F. Brown, J. Amer. Chem. Soc. **74,** 2534 (1952); **74,** 2538 (1952).
[6] P. Gross, H. Steiner, and F. Krauss, Trans. Faraday Soc. **32,** 877 (1936). – J. C. Hornell and J. A. V. Butler, J. Chem. Soc. **1936,** 1361.
[7] V. Gold, Trans. Faraday Soc. **56,** 255 (1960); Adv. Phys. Org. Chem. **7,** 259 (1969).
[8] A. J. Kresge, Pure Appl. Chem. **8,** 243 (1964).
[9] J. P. Elrod, R. D. Gandour, J. L. Hogg, M. Kise, G. M. Maggiora, R. L. Schowen, and K. S. Venkatasubban, Faraday Symp. Chem. Soc. **10,** 145 (1975).
[10] J. D. Hermes and W. W. Cleland, J. Amer. Chem. Soc. **106,** 7263 (1984).
[11] J. D. Hermes, S. W. Morrical, M. H. O'Leary, and W. W. Cleland, Biochemistry **23,** 5479 (1984).
[12] J. G. Belasco, W. J. Albery, and J. R. Knowles, Biochemistry **25,** 2529 (1986); **25,** 2552 (1986).
[13] M. Ek, P. Ahlberg, Chemica Scripta **16,** 62 (1980). – K. A. Engdahl, H. Bivehed, P. Ahlberg, and W. H. Saunders Jr., J. Chem. Soc. Chem. Comm. **1982,** 42.
[14] S. Glasstone, K. J. Laidler, and H. Eyring, The Theory of Rate Processes, McGraw-Hill, New York 1941.
[15] L. Waldmann, Naturwiss. **31,** 205 (1943). – J. Bigeleisen and M. Goeppert Mayer, J. Chem. Phys. **15,** 261 (1947). – J. Bigeleisen, J. Chem. Phys. **23,** 2264 (1955).
[16] J. Bigeleisen, J. Chem. Phys. **17,** 675 (1949).
[17] H. H. Limbach, J. Hennig, D. Gerritzen, and H. Rumpel, Faraday Disc. Chem. Soc. **74,** 229 (1982).
[18] W. J. Albery and H. H. Limbach, J. Chem. Soc. Faraday Discussion **24,** 291 (1982).
[19] W. J. Albery, J. Phys. Chem. **90,** 3773 (1986).
[20] D. Gerritzen and H. H. Limbach, Ber. Bunsenges. Phys. Chem. **85,** 527 (1981).
[21] D. Geritzen and H. Limbach, J. Amer. Chem. Soc. **106,** 869 (1984).
[22] H. H. Limbach, J. Magn. Reson. **36,** 287 (1979).
[23] H. H. Limbach and W. Seiffert, J. Amer. Chem. Soc. **102,** 538 (1980).
[24] D. Gerritzen and H. H. Limbach, J. Phys. Chem. **84,** 799 (1980).
[25] H. H. Limbach, J. Hennig, and J. Stulz, J. Chem. Phys. **78,** 5432 (1983).
[26] J. Hennig and H. H. Limbach, J. Amer. Chem. Soc. **106,** 292 (1984).
[27] J. Hennig and H. H. Limbach, J. Magn. Reson. **49,** 322 (1982).
[28] M. Schlabach, B. Wehrle, H. H. Limbach, E. Bunnenberg, A. Knierzinger, A. Shu, B. R. Tolf, and C. Djerassi, J. Amer. Chem. Soc. **108,** 3856 (1986).
[29] G. Otting, H. Rumpel, L. Meschede, G. Scherer, and H. H. Limbach, Ber. Bunsenges. Phys. Chem. **90,** 1122 (1986).
[30] H. H. Limbach and D. Gerritzen, J. Chem. Soc. Faraday Disc. **74,** 279 (1982).
[31] L. Meschede, D. Gerritzen, and H. H. Limbach, Ber. Bunsenges. Phys. Chem. **92,** 469 (1988).
[32] H. Rumpel, H. H. Limbach, G. Zachmann, J. Phys. Chem. **93,** 1812 (1989).
[33] H. Rumpel and H. H. Limbach, J. Amer. Chem. Soc., in press.
[34] M. Schlabach, H. Rumpel, and H. H. Limbach, Angew. Chemie **101,** 84 (1989); Angew. Chem. Int. Ed. Engl. **28,** 76 (1989). – T. Butenhoff and C. B. Moore, J. Amer. Chem. Soc. **110,** 8336 (1988).
[35] H. H. Limbach, J. Hennig, R. D. Kendrick, and C. S. Yannoni, J. Amer. Chem. Soc. **106,** 4059 (1984).
[36] H. H. Limbach, D. Gerritzen, H. Rumpel, B. Wehrle, G. Otting, H. Zimmermann, R. D. Kendrick, and C. S. Yannoni, in: Photoreaktive Festkörper (H. Sixl, J. Friedrich, and C. Bräuchle, eds.), M. Wahl Verlag, Karlsruhe 1985, p. 19.
[37] R. D. Kendrick, S. Friedrich, B. Wehrle, H. H. Limbach, and C. S. Yannoni, J. Magn. Reson. **65,** 159 (1985).
[38] H. H. Limbach, B. Wehrle, H. Zimmermann, R. D. Kendrick, and C. S. Yannoni, J. Amer. Chem. Soc. **109,** 929 (1987).
[39] H. H. Limbach, B. Wehrle, H. Zimmermann, R. D. Kendrick, and C. S. Yannoni, Angew. Chem. **99,** 241 (1987); Angew. Chem. Int. Ed. Eng. **26,** 247 (1987).
[40] B. Wehrle, H. H. Limbach, M. Köcher, O. Ermer, and E. Vogel, Angew. Chem. **99,** 914 (1987); Angew. Chem. Int. Ed. Eng. **26,** 935 (1987).
[41] B. Wehrle, H. Zimmermann, and H. H. Limbach, Ber. Bunsenges. Phys. Chem. **91,** 941 (1987).
[42] B. Wehrle, H. Zimmermann, and H. H. Limbach, J. Amer. Chem. Soc. **110,** 7014 (1988).

[43] B. Wehrle, F. Aguilar-Parrilla, H. H. Limbach, M. Foces-Foces, F. H. Cano, J. Elguero, A. Baldy, M. Pierrot, M. M. T. Kurshid, J. B. Larcombe-McDuall, and J. A. S. Smith, J. Amer. Chem. Soc., in press.
[44] A. Claisen, Lieb. Ann. Chem. **287,** 366 (1895). – G. Heller, Chem. Ber. **37,** 3116 (1904).
[45] N. E. White and M. Kilpatrik, J. Phys. Chem. **59,** 1044 (1955).
[46] H. U. Sieveking and W. Lüttke, Lieb. Ann. Chem. 189 (1977).
[47] J. D. Halliday, E. A. Symons, and P. E. Bindner, Can. J. Chem. **56,** 1470 (1978).
[48] E. V. Borisov, D. N. Kratsov, A. S. Peregudov, and E. I. Fedin, Izv. Akad. Nauk SSSR, Ser. Khim. 2151 (1980).
[49] D. G. Ott, Synthesis with Stable Isotopes, John Wiley & Sons, New York, Toronto 1981.
[50] G. Schiemann and H. G. Baumgarten, Chem. Ber. **70,** 1416 (1937).
[51] T. Axenrod, P. S. Pregosin, M. J. Wieder, E. D. Becker, R. B. Bradley, and G. W. A. Milne, J. Amer. Chem. Soc. **93,** 6536 (1971).
[52] C. Carvajal, K. J. Tölle, J. Smid, and M. Swarc, J. Amer. Chem. Soc. **87,** 5548 (1965). – D. J. Metz and A. Glines, J. Phys. Chem. **71,** 1158 (1967).
[53] W. Marquardt, Share Distribution Center, Program No. 1428 (1964).
[54] R. Kubo, Nuovo Cimento, Suppl. 6, 1063 (1957). – R. A. Sack, Mol. Phys. **1,** 163 (1958).
[55] S. Alexander, J. Chem. Phys. **37,** 971 (1962).
[56] G. Binsch, J. Amer. Chem. Soc. **91,** 1304 (1969).
[57] R. R. Ernst, G. Bodenhausen, and A. Wokaun, Principles of Nuclear Magnetic Resonance in One and Two Dimensions. Clarendon Press, Oxford 1987.
[58] K. M. Merz and C. H. Reynolds, J. Chem. Soc. Chem. Comm. 90 (1988).
[59] Z. Smedarchina, W. Siebrand, and T. A. Wildmann, Chem. Phys. Lett. **143,** 395 (1988).
[60] A. Novak, Struct. Bond. **14,** 177 (1974).